Localization of light in disordered dielectrics: An approach based on spectral statistics

Markus Saltzer* and Hans A. Weidenmüller
Max-Planck-Institut für Kernphysik, Postfach 103980, 69029 Heidelberg, Germany
(Received 22 October 1999)

We study numerically the fluctuation properties of the eigenvalues of the scalar wave equation in two dimensions for strong disorder. This equation mimicks properties of light in dielectrics. With increasing disorder, we find a transition from diffusive to localized behavior, in complete analogy to the case of Schrödinger waves (electrons). At low frequencies, we observe a suppression of disorder. This effect is caused by the wave number dependence of the disorder term in the wave equation, and has no analog in the case of electrons.

PACS number(s): 42.25.Dd, 05.60.−k, 78.20.Bh

I. INTRODUCTION AND MOTIVATION

During the last decade, the propagation of waves through disordered media has been studied intensely. Surprising similarities between the transport of electrons (i.e., Schrödinger waves) in disordered solids and that of light waves in random dielectrics have been revealed. Examples are universal conductance fluctuations and weak localization for electrons [1] versus long-range correlations in speckle patterns [2] and coherent backscattering for light [3], respectively; see also Ref. [4]. Recently, direct experimental evidence for the analog of Anderson localization of electrons in disordered solids [5] was reported for light [6,7].

These experimental results go along with a growing theoretical understanding of the similarities and differences between the two classes of phenomena. Early work applied the diagrammatic perturbation theory successfully developed for electrons to the calculation of properties of speckle patterns which were shown to be analogs of the universal conductance fluctuations. Later, Efetov's nonlinear supersymmetric σ model [8] emerged as the generic model for equilibrium and transport phenomena in disordered media. This model was originally developed for noninteracting electrons in disordered solids. It applies in the limit of weak disorder. Here it provides a link between spectral fluctuation and transport properties, and between random-matrix theory (RMT) and localization theory. The Thouless energy which limits the range of validity of RMT appears naturally in the model. Moreover, the model allows for the calculation of nonperturbative results; see Ref. [9]. Recently, the model was extended to the case of transport of classical waves (light) through a disordered medium [10–12]. It was shown that the effective Lagrangians governing electrons in disordered solids and classical waves in a disordered medium are identical, and that only the source terms differ. This was somewhat surprising because Schrödinger waves and classical waves possess different Ward identities [4].

While we do possess a generic theoretical model and a fairly comprehensive understanding of the associated phenomena in the weak disorder limit, the same cannot be said of the case of strong disorder. Indeed, there is no adequate theoretical framework which would cover this case, and one has to resort to numerical simulation. This is what we do in this paper. Rather than studying a transport property, we investigate the spectral fluctuation properties of classical waves (light) in a strongly disordered dielectric. In order to test the influence of disorder and to define the transition to localization, we apply the usual measures (the nearest neighbor spacing distribution and the Δ_3 statistic) to the eigenvalue distribution. A comparison with the case of electrons serves as a test for the equivalence between electrons and classical waves in this regime.

The propagation of light in a disordered medium is described by the scalar wave equation

$$[\,-\Delta+\delta\epsilon(\vec{r})k^2\,]\,\Phi=\epsilon_0 k^2\,\Phi. \tag{1}$$

Here $k=\omega/c$ is the wave number. The space dependent dielectric constant $\epsilon(\vec{r})=\epsilon_0-\delta\epsilon(\vec{r})$ is decomposed into a space independent background term ϵ_0 and a fluctuating part $\delta\epsilon(\vec{r})$. As a response variable, the dielectric constant $\epsilon(\vec{r})$ has to be positive. Therefore, $|\delta\epsilon(\vec{r})|<\epsilon_0$. The fluctuating part $\delta\epsilon(\vec{r})$ is assumed to be a random process with vanishing first moment, and a second moment given by

$$\langle\delta\epsilon(\vec{r}_1)\,\delta\epsilon(\vec{r}_2)\rangle=\frac{4\pi}{l k_0^{d+1}}\,\delta(\vec{r}_1-\vec{r}_2). \tag{2}$$

Here l is the elastic mean free path, d is the dimension of the system, and k_0 is a suitably chosen wave number to be discussed below. Comparing the scalar wave equation (1) with the Schrödinger equation for an electron with energy E in a disorder potential V, we note the formal correspondence between $\epsilon_0 k^2$ and the energy E, and between $\delta\epsilon(\vec{r})k^2$ and the potential V. Differences between the two wave equations are due to two facts: (i) Since $\epsilon_0 k^2$ is always positive while E is not, there is no analog of bound states of the Schrödinger equation for light. (ii) More importantly, the random term $\delta\epsilon(\vec{r})k^2$ in Eq. (1) is proportional to k^2 while V is independent of energy. This second difference has far-reaching consequences [13,10].

*Present address: Fakultät für Physik, Universität Freiburg, Hermann-Herder-Strasse 3, 79104 Freiburg, Germany.

Equation (2) is written [11] in complete analogy to the case of electrons where a formally identical relation holds, and where k_0 is given by the Fermi energy. This equation guarantees that in the weak-coupling case and for $k=k_0$, the parameter controlling the exponential decay of the average Green function is indeed l. Thus Eq. (2) serves as the link between l and the variance of the impurity scattering potential. However, Eq. (2) obviously does not imply an additional and unphysical energy dependence of $\delta\epsilon$. This is why k_0 must be held fixed, and must not be identified with the actual wave number k.

Two views may be held regarding the relevance of Eq. (2) in the case of light scattering. (i) One may consider $\delta\epsilon$ the primary physical quantity and l a derived one. In this case, one would keep the variance of $\delta\epsilon$, i.e., the value of the constant lk_0^{d+1} in Eq. (2), fixed over the entire range of frequencies studied in the numerical simulation. By adopting a set of values of k_0 in this frequency range, one would then find a corresponding set of l values, one for each value of k_0 and the associated frequency interval. (ii) If, on the contrary, l is the primary physical quantity and $\delta\epsilon$ the derived one, one would keep l fixed. Then, Eq. (2) would apply in a sufficiently small interval of wave numbers centered on k_0, and one would have to readjust the variance of $\delta\epsilon$ as one sweeps over a large frequency interval.

In the case of electrons, the condition for strong disorder reads $kl\approx 1$. For light, strong disorder effects like Anderson localization are similarly expected to occur whenever the transport mean free path is of the order of the wavelength. This suggests that the quantity of primary interest for localization is the elastic mean free path l rather than the variance of the disorder term $\delta\epsilon$. We organize our numerical calculations accordingly.

Confining ourselves to two dimensions, we will show that with increasing disorder our model exhibits a transition from extended to localized states, in qualitative agreement with the case of electrons. A significant difference is due to the explicit k^2 dependence of the disorder term: With increasing wavelength $\lambda=2\pi/k$, disorder becomes more and more suppressed. Thus the condition $\lambda\approx l$ is, for small values of k, no longer a sufficient condition for localization.

It has been known for some time that in one-dimensional systems, the localization length for a wave equation with a random index of refraction diverges at the boundary $k=0$ of the spectrum. This fact is related to the stability of the boundary with respect to impurity concentration [14]. The divergence was obtained directly in Ref. [15], and can also be deduced from corresponding results for electrons using a duality relation connecting low energy behavior of the wave equation and high energy behavior of the Schrödinger equation [16]. In this sense, the results presented below extend existing knowledge but do not come as a big surprise.

The paper is organized as follows. In Sec. II we introduce the numerical model. The results of the spectral fluctuation analysis are presented in Sec. III, where we also compare our results to the case of electrons. Our conclusions are drawn in Sec. IV.

II. MODEL

Discretization of Eq. (1) leads to an eigenvalue equation of the form

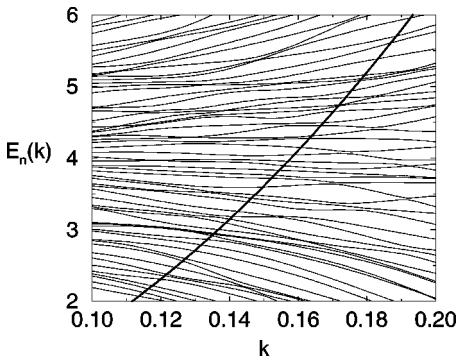

FIG. 1. Interpolating curves vs wave number k (in units of the lattice constant a) for a sequence of eigenvalues $E_n(k)$, $n=1,2,\ldots$, for a lattice of size $L=10$ with 100 sampling points per eigenvalue. The curve $\epsilon_0 k^2$ is plotted as a thick solid line. The points of intersection of $\epsilon_0 k^2$ with the $E_n(k)$'s give the solutions of Eq. (3).

$$H(k)\,|\Phi\rangle=\epsilon_0 k^2\,|\Phi\rangle, \tag{3}$$

with an energy dependent Hamiltonian written in Dirac notation as

$$H(k)=\sum_i\,(k^2\delta\epsilon_i+2d)\,|i\rangle\langle i|-\sum_{\langle i,j\rangle}|i\rangle\langle j|. \tag{4}$$

The states $|i\rangle$ belong to the sites of a d-dimensional lattice of length L_0. The sum $\langle i,j\rangle$ is taken over nearest neighbors only. The wave number k and all other length-dependent quantities are written in units of the lattice constant a, where a is set equal to unity so that $k=ka$ and $l=l/a$ with $a=1$. We restrict ourselves to $d=2$ and choose periodic boundary conditions. The independent random variables $\delta\epsilon_i$ are equally distributed in the interval $[-W/2,W/2]$. On account of Eq. (2) we obtain $W/2=\sqrt{12\pi/lk_0^3}$. The important difference between Eq. (4) and the standard tight-binding Hamiltonian lies in the dependence of the random term on the wave number k^2 (this dependence causes an ''energy dependence'' of the ''disorder potential'' which is absent in the case of electrons).

The restriction to $d=2$ is necessary to simplify the numerical effort. However, it has one unphysical consequence. The scaling of the random variable introduced in Eq. (2) depends on dimension and implies that, for $d=2$, the quantity $\langle(\delta\epsilon k_0^2)^2\rangle$ is proportional to k_0 while in $d=3$ it would be independent of k_0. Put differently, the map $l\Leftrightarrow\delta\epsilon$ depends on dimension d. This fact has to be kept in mind when we discuss our results.

We solve Eq. (3) by first calculating the eigenvalues $E_n(k')$ for Hamiltonian (4) for a set of fixed wave numbers k', and for a fixed realization of the random variables $\delta\epsilon_i$. For each integer n we interpolate $E_n(k')$ plotted over the sampling points k' along the k axis to obtain a numerical function $E_n(k)$. The condition $\epsilon_0 k^2=E_n(k)$ leads directly to the graphical solutions k_n^2 of Eq. (3). This procedure is demonstrated in Fig. 1. Because of the occurrence of avoided crossings in the $E_n(k)$, we pay special attention to the sampling resolution along the k axis. The choice of too few sampling points k' will smear out the curves $E_n(k)$ and, therefore, will distort the results. On the other hand, improving

the resolution affects the number of diagonalizations to be carried out and, hence, the computing time. The problem is compounded by the need to average over a sufficient number of realizations of the set of random variables $\delta\epsilon_i$. Typically, we have generated 250 realizations of the ensemble. Thus the need to attain high numerical resolution restricts us to small system sizes. The systems under study in this paper are mostly of size 20×20.

In the following we present two series of data sets. In both cases, the variance of $\delta\epsilon$ is fixed by choosing l and k_0, and is given by

$$\langle \delta\epsilon_i \delta\epsilon_j \rangle = \frac{4\pi}{l k_0^{d+1}} \delta_{ij}. \tag{5}$$

First we approach the condition $\lambda \approx l$ at a fixed wavelength λ_0 (we choose the wave number $k_0 = 1.064$) by decreasing the elastic mean free path l, with $l = 5$, 3, and 1.4098. The disorder parameters are then $k_0 l = 5.32$, 3.192, and 1.5. In the second series, we compare waves of different energies by decreasing the wave number k_0 but keeping l fixed. Beginning with the last configuration ($l = 1.4098$ and $k_0 = 1.5$) of the first series, we proceed with $k_0 = 0.9$ and 0.8. The disorder parameter is then reduced further, $k_0 l = 1.5$, 1.269, and 1.128. In both cases, our results are meaningful for k values in the vicinity of k_0.

In reducing the disorder parameter $k_0 l$, we must increase the dielectric constant ϵ_0. This is because small values of $k_0 l$ imply large values of $\delta\epsilon_i$, cf. Eq. (5), which in turn through the condition $|\delta\epsilon_i| < \epsilon_0$ affects the minimum acceptaple value of ϵ_0. There are two reasonable choices for the dielectric constant which are consistent with this requirement. (i) ϵ_0 is held fixed for a series of calculations, or (ii) ϵ_0 is defined dynamically as the maximum value of the $\delta\epsilon_j$'s occurring in the simulation. In the first case one is automatically restricted to values of the parameters l and k_0 which lie above certain bounds given by the condition $|\delta\epsilon_i| < \epsilon_0$. This does not happen in the second case, where the fluctuations of the total dielectric constant lie in the interval $[0, 2\epsilon_0]$. Actually, the two cases are not very different, and have qualitatively the same effect. This is seen by applying the transformation $\vec{s} = \sqrt{\epsilon_0}\vec{r}$ to Eq. (1). We found it simpler to use the dynamical determination of ϵ_0, leading to the values $\epsilon_0 = 2.502$, 3.32, and 4.712 for the sequence $l = 5$, 3, and 1.4098, respectively, and $\epsilon_0 = 4.712$, 6.075, and 7.227 for the sequence $k_0 = 1.064$, 0.9, and 0.8, respectively.

III. DATA ANALYSIS

In Sec. III A we describe the unfolding of the spectra, and in Secs. III B and in III C we show the nearest neighbor spacing distribution and the spectral two-point correlation function, respectively. The latter allows us to identify the Thouless energy and, thus, the domain of validity of RMT. The results are discussed in Sec. III D.

A. Unfolding

The unfolding procedure removes the influence of a nonconstant mean level density on the spectral fluctuation properties. Our calculations yield an ordered sequence of ''eigenvalues,'' specified in terms of the wave numbers $k_1, k_2, \ldots, k_N$. We recall that the cumulative spectral function or staircase function,

$$\eta(k) = \int_{-\infty}^{k} dk' \sum_{n=1}^{N} \delta(k' - k_n) = \sum_{n=1}^{N} \Theta(k - k_n), \tag{6}$$

counts the number of levels with wave number $\leqslant k$. This function is decomposed into an average part $\eta_{\rm av}(k)$ and a fluctuating part $\eta_{\rm fluc}(k)$:

$$\eta(k) = \eta_{\rm av}(k) + \eta_{\rm fluc}(k). \tag{7}$$

The spectrum is unfolded by mapping the sequence $k_1, \ldots, k_N$ onto the sequence $\xi_1, \ldots, \xi_N$, with

$$\xi_n = \eta_{\rm av}(k_n). \tag{8}$$

In the unfolded spectrum the mean level density is unity.

We have determined the average staircase function $\eta_{\rm av}(k)$ by averaging over the ensemble of sequences $k_1, \ldots, k_N$ generated in the calculation [17]. To this end, we have divided the relevant range of wave numbers into M bins labeled $i = 1, \ldots, M$ with common widths Δk. In each bin $i, (i = 1, \ldots, M)$, we calculated the average level density ρ_i as an average over the ensemble of sequences generated in the calculation. The average part of the cumulative spectral function is then obtained by a summation over bins,

$$\eta_{\rm av}(\kappa) = \sum_{i=1}^{j} \rho_i, \tag{9}$$

where κ is the k value corresponding to the right-hand side border of bin number j. An interpolation between the κ values then gives $\eta_{\rm av}(k)$ for all k.

The fluctuation measures displayed in the following sections have likewise been calculated as ensemble averages. For the case of the nearest-neighbor spacing distribution, this was done at a fixed value of k given by k_0. In the case of the two-point correlation function, a neighborhood of k_0 was used.

B. Nearest neighbor spacing distribution

The nearest neighbor spacing distribution $p(s)$ is the observable most commonly used to study short-range fluctuations in a spectrum. It is the probability density of finding a distance s between adjacent levels on the unfolded scale. For the Gaussain orthogonal ensemble of random matrices (GOE, the relevant ensemble in our case), Wigner surmised for $p(s)$ the shape

$$p(s) = \frac{\pi}{2} s \exp\left(-\frac{\pi}{4} s^2 \right), \tag{10}$$

which is very close to the exact result. In the case of completely uncorrelated levels $p(s)$ is given by the Poisson distribution

$$p(s) = \exp(-s). \tag{11}$$

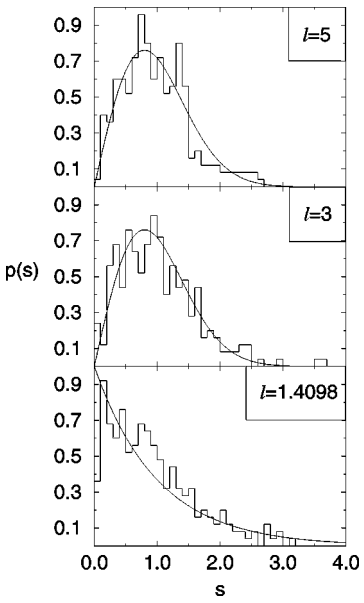

FIG. 2. Nearest neighbor spacing distribution $p(s)$ for the series of data sets with $l=5$, 3, and 1.4098 at $k_0=1.064$. The solid lines are GOE and Poisson predictions, respectively.

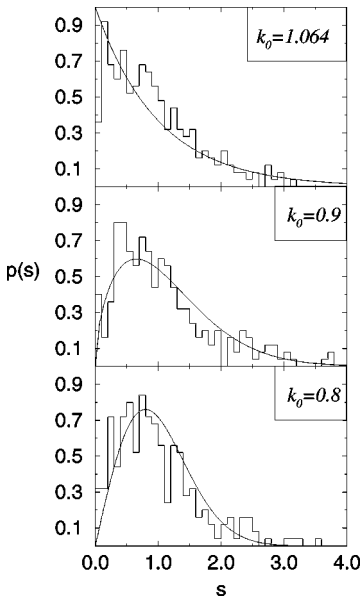

FIG. 3. Nearest neighbor spacing distribution $p(s)$ for the series of data sets with $k_0=1.5$, 0.9, and 0.8 at $l=1.4098$. The solid lines are Poisson and GOE predictions, respectively. For $k_0=0.9$ the data are fitted with the Brody distribution; see the text.

Both the GOE and the Poisson distribution are shown as solid lines in Fig. 2 (upper and middle panel: GOE; lower panel: Poisson).

Figure 2 shows our numerical results for the first series of data sets. We recall that we consider three different disorder parameters $k_0 l=5.32$, 3.192, and 1.5 at a fixed wave number $k_0=1.064$, corresponding to mean free path values $l=5$, 3, and 1.4098. The nearest neighbor spacing distribution exhibits a transition from GOE behavior for the largest mean free path, i.e., relatively weak disorder, to a Poisson distribution for the smallest mean free path, i.e., strong disorder. We recall that in the second data set, we leave the mean free path l fixed at $l=1.4098$ and vary the wave number $k_0=1.5$, 0.9, and 0.8, so that $k_0 l=1.5$, 1.269, and 1.128. The data are shown in Fig. 3. We observe a transition from the Poisson distribution to GOE statistics. The data set with $k_0=0.9$ has been fitted with the ''Brody distribution'' [18]

$$p_q(s)=c_q s^q \exp\left(-\frac{c_q s^{q+1}}{q+1}\right) \tag{12}$$

with $c_q=[\Gamma^{q+1}(1/(q+1))]/(q+1)$ and $0\leqslant q\leqslant 1$. This gives $q\approx 0.55$ for the mixture between the Wigner surmise and the Poisson distribution (the solid curve in the middle of Fig. 3).

C. Two-point spectral correlations

Correlations between pairs of spacings are studied with the help of the number variance $\Sigma^2(L)$ and the spectral rigidity $\Delta_3(L)$. We recall the definitions [19]. The number variance is given by

$$\Sigma^2(L)=\langle [L-n(L,\xi_{k_0})]^2\rangle. \tag{13}$$

Here $n(L,\xi_{k_0})$ counts the number of levels in the interval $[\xi_{k_0},\xi_{k_0}+L]$ on the unfolded scale. For an uncorrelated (Poisson) spectrum we have $\Sigma^2(L)=L$ and for the GOE, $\Sigma^2(L)\sim\log(L)$. The average in Eq. (13) is taken over the ensemble at fixed energy ξ_{k_0}. The spectral rigidity is given by

$$\Delta_3(L)=\left\langle \frac{1}{L}\min_{A,B}\int_{\xi_{k_0}}^{\xi_{k_0}+L} d\xi[\,\eta(\xi)-A\xi-B]^2\right\rangle. \tag{14}$$

The average is again taken over the ensemble. The function $\Delta_3(L)$ can be expressed as an integral over the number variance and is, therefore, smoother than $\Sigma^2(L)$.

The results for the two series of data sets are shown in Figs. 4 and 5. In both cases, the numerical data agree with the GOE prediction up to a certain point and then tend to deviate from it linearly. This allows us to determine the Thouless energy approximately as the point of departure from GOE behavior. Starting with a disorder parameter $k_0 l=5.32$ at $l=5$ in Fig. 4, we observe that with decreasing mean free path l, the Thouless energy shrinks all the way down to a value close to the mean level spacing. For $k_0 l=1.5$, i.e., $l=1.4098$, we do not even find any GOE behavior in the level number variance anymore. The correlations are very close to Poisson-type behavior. Figure 5 shows a Poisson-like distribution at values $k_0 l=1.5$ and $k_0=1.064$. Keeping the mean free path l fixed and decreasing the wave number k_0 we observe a transition back to GOE-type statistics. In order to give a better illustration of the transition, we also show the correlation functions for $k_0=0.5$.

D. Discussion

Before discussing our results we recall some pertinent facts about level statistics of noninteracting electrons in disordered mesoscopic solids [9]. We consider a situation where the size L_0 of the system is large compared to the elastic mean free path l. The diffusive regime ($L_0\ll\xi$) and the lo-

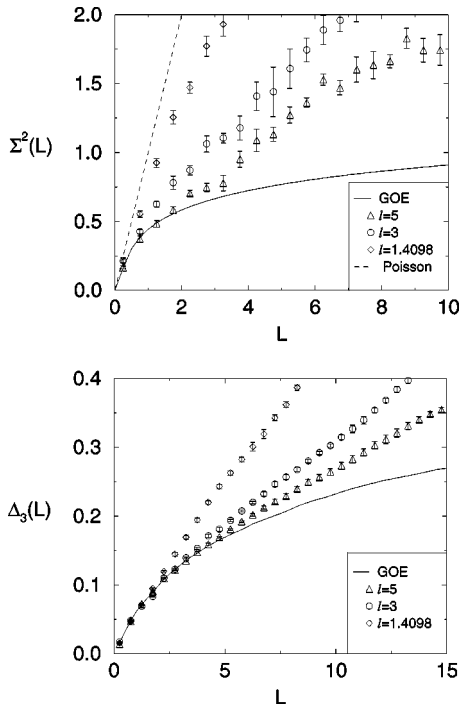

FIG. 4. Level number variance $\Sigma^2(L)$ and spectral rigidity $\Delta_3(L)$ for $l=5$, 3, and 1.4098 at $k_0=1.064$. The GOE and Poisson predictions are plotted as solid and dashed lines, respectively.

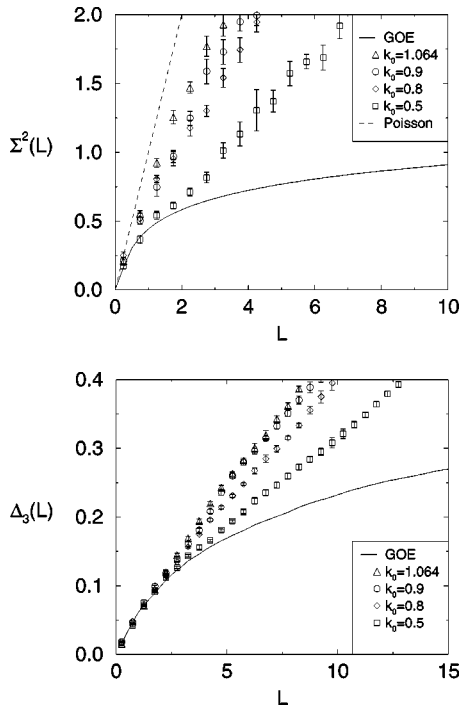

FIG. 5. Level number variance $\Sigma^2(L)$ and spectral rigidity $\Delta_3(L)$ for $k_0=1.5$, 0.9, and 0.8, and 0.5 at $l=1.4098$. The GOE and Poisson predictions are plotted as solid and dashed lines, respectively.

calized regime ($L_0 \gg \xi$) are distinguished by comparing the length L_0 with the localization length ξ. In the diffusive regime, the states are extended, and the level statistics follows RMT up to a critical energy, the Thouless energy E_c [20,21]. Beyond this scale, the two-point spectral correlation function follows a power law, i.e., grows $\sim L^{d/2}$. The Thouless energy also defines the transition to localization: This transition occurs when E_c as a function of some system parameter decreases and becomes of the order of the mean single-particle level spacing.

We turn to the first series of data sets shown in Secs. III B and III C, i.e., to the sequence where k_0 is held fixed and l is decreased. The nearest neighbor spacing distribution displays a transition from a GOE-type distribution to a Poissonian one. The two-point correlation functions give a more differentiated picture. For $l=5$ we do find GOE behavior for small values of L, and an approximately linear growth for large values of L. This linear growth is in perfect agreement with the case of electrons (we recall $d=2$). The Thouless energy marking the transition between both regimes is seen to decrease with decreasing l. For $l=3$ the two–point correlation functions already signal a transition to a Poisson-like, statistic while the nearest neighbor spacing distribution still shows Wigner-Dyson statistics. At $l=1.4098$ both the two-point correlation functions and the nearest neighbor spacing distribution are practically Poisson distributed, and indicate localization. Thus enhancement of the disorder by a decrease of the mean free path causes a classical wave with fixed wave number to undergo Anderson localization, in complete analogy to the case of electrons.

The second series of data sets probes the dependence of the level statistics on the wave number in two dimensions. We find that for a fixed value of the mean free path l, a decrease of the wave number k_0 causes a transition from a Poisson distribution to GOE-like behavior. At first sight, this result is surprising because a decrease of k_0 amounts to a decrease of the disorder parameter. We attribute this result to the fact mentioned in Sec. II: For $d=2$, the quantity $\langle(\delta\epsilon k_0^2)^2\rangle$ is proportional to k_0, and, thus, diminishes as we reduce k_0. The transition from localized back to extended states suggested by the data therefore reflects a transition from a strongly disordered to a more weakly disordered scattering medium. This transition clearly occurs in the scalar wave equation only and has no analog for Schrödinger waves. For the reasons discussed in Sec. II, it is possible that the effect is much stronger for $d=2$ than it is for $d=3$. But we expect a similar behavior there, too, at sufficiently small wave numbers, caused by the k^2 dependence of the disorder term.

IV. SUMMARY AND CONCLUSION

We have numerically studied scalar waves in a disordered medium in two dimensions. By investigating the spectral fluctuations, we have shown that a classical wave of fixed wavelength becomes localized for sufficiently strong disorder, in complete analogy to the case of electrons in a disordered medium. The main difference between the wave equations for classical and Schrödinger waves lies in the energy dependence of the disorder potential and emerges when we compare the spectral statistics of classical waves of different wavelengths in the limit of long wavelength. In our two-dimensional system we observe an increasing suppression of disorder effects at low frequencies. This does not happen for electrons, and relates to the frequency dependence of the scattering cross section which is found for light but not for

electrons. The fact that the calculations were done in two dimensions may overemphasize the effect but the same kind of phenomenon is expected to occur in three dimensions on a somewhat reduced scale.

One-parameter scaling has been used to show that in two dimensions, electrons are localized for any disorder [22]. Do our results imply that this statement does not hold for the wave equation? We cannot answer this question in full: Our simulation is necessarily limited to a finite two-dimensional area. We have shown that the boundary of the spectrum at $k=0$ has a profound impact on the localization length. However, we cannot exclude the possibility that the localization length becomes very large at the boundary without actually diverging.

[1] Y. Imry, *Introduction to Mesoscopic Physics* (Oxford University Press, New York, 1997).

[2] F. Scheffold and K G. Maret, Phys. Rev. Lett. **81**, 5800 (1998).

[3] M. P. van Albada and A. Lagendijk, Phys. Rev. Lett. **55**, 2692 (1985); P. E. Wolf and G. Maret, *ibid.* **55**, 2696 (1985).

[4] P. Sheng, *Introduction to Wave Scattering, Localization, and Mesoscopic Phenomena* (Academic Press, San Diego, 1995).

[5] P. W. Anderson, Philos. Mag. B **52**, 505 (1985).

[6] D. S. Wiersma, P. Bartolini, A. Lagendijk, and R. Righini, Nature (London) **390**, 671 (1997).

[7] F. J. P. Schuurmans, M. Megens, D. Vanmaekelbergh, and A. Lagendijk, Phys. Rev. Lett. **87**, 2183 (1999).

[8] K. B. Efetov, Adv. Phys. **32**, 53 (1983).

[9] T. Guhr, A. Müller-Groeling, and H. A. Weidenmüller, Phys. Rep. **299**, 189 (1998).

[10] B. Elattari, V. Kagalowski, and H. A. Weidenmüller, Phys. Rev. E **57**, 2733 (1997).

[11] B. Elattari, V. Kagalovsky, and H. A. Weidenmüller, Phys. Rev. B **57**, 11 258 (1998).

[12] B. Elattari, V. Kagalovsky, and H. A. Weidenmüller, Europhys. Lett. **42**, 13 (1998).

[13] A. Lagendijk and B. A. van Tiggelen, Phys. Rep. **270**, 143 (1996).

[14] I. M. Lifshitz, Adv. Phys. **13**, 483 (1964).

[15] J. B. Keller, G. C. Papanicolaou, and J. Weilenmann, Commun. Pure Appl. Math. **32**, 583 (1978).

[16] S. A. Gredeskul, A. V. Marchenko and L. A. Pastur, *Surveys in Applied Mathematics* (Plenum Press, New York, 1995), Vol. 2, p. 63.

[17] T. Guhr, J.-Z. Ma, S. Meyer, and T. Wilke, Phys. Rev. D **59**, 054501 (1999).

[18] T. A. Brody, Lett. Nuovo Cimento **7**, 482 (1973).

[19] M. L. Mehta, *Random Matrices*, 2nd ed. (Academic Press, New York, 1991).

[20] D. J. Thouless, J. Phys. C **8**, 1803 (1975).

[21] D. J. Thouless, Phys. Rev. Lett. **39**, 1167 (1977).

[22] E. Abrahams, P. W. Anderson, P. A. Lee, and T. V. Ramakrishnan, Phys. Rev. B **24**, 6783 (1982).